DIANet: Dense-and-Implicit Attention Network

Zhongzhan Huang[*]
New Oriental AI Research Academy, Haidian, Peking
Tsinghua University, Haidian, Peking
hzz17@mails.tsinghua.edu.cn

Senwei Liang[*]
National University of Singapore
10 Lower Kent Ridge Road
liangsenwei@u.nus.edu

Mingfu Liang
Northwestern University
Evanston, Illinois
mingfuliang2020@u.northwestern.edu

Haizhao Yang [†]
National University of Singapore
10 Lower Kent Ridge Road
matyh@nus.edu.sg

Abstract

Attention-based deep neural networks (DNNs) that emphasize the informative information in a local receptive field of an input image have successfully boosted the performance of deep learning in various challenging problems. In this paper, we propose a Dense-and-Implicit-Attention (DIA) unit that can be applied universally to different network architectures and enhance their generalization capacity by repeatedly fusing the attention throughout different network layers. The communication of attention between different layers is carried out via a modified Long Short Term Memory (LSTM) module within the DIA unit that is in parallel with the DNN. The sharing DIA unit links multi-scale features from different depth levels of the network implicitly and densely. Experiments on benchmark datasets show that the DIA unit is capable of emphasizing channel-wise feature interrelation and leads to significant improvement of image classification accuracy. We further empirically show that the DIA unit is a nonlocal normalization tool that enhances the Batch Normalization.

1 Introduction

Attention, a cognitive process that selectively focuses on a small part of information while neglects other perceivable information[1], has been used to effectively ease neural networks from learning large information contexts from images [2, 3], sentences [4, 5, 6] and videos [7]. Especially in computer vision, DNNs incorporated with special operators that mimic the attention mechanism can process informative regions in an image efficiently. Empirical results in [8, 9, 2, 10, 4, 11] have demonstrated the improvement of DNNs' visual representations [12] by these special attention operators. Recently, attention operators are modularized and stacked into popular networks as attention modules [13, 14] for further performance improvement. The design of these modules may be task-dependent. [15, 16, 17, 18, 12, 19, 20].

In previous works, attention-modules are used individually in each layer throughout DNNs. Even a tiny add-in module with a small amount of parameters per layer will primarily increase the total number of parameters as the network depth increases. Besides, the potential network redundancy can also hinder the learning capability of DNNs [14, 21]. Therefore, it is crucial to design efficient attention modules that can maintain reasonable parameter cost and avoid feature redundancy to improve the performance of DNNs.

---

[*]Equal contribution
[†]Corresponding author

1.1 Our contribution

To tackle the challenge mentioned above, we propose a Dense-and-Implicit Attention (DIA) unit to enhance the generalization capacity of DNNs. The DIA unit can recurrently fuse network attention from previous network layers to latter network layers. The structure and computation flow of a DIA unit is visualized in Figure 1. There are three parts in the DIA unit. The part denoted by ① extracts spatial-wise [22], channel-wise [15] or multi-scale features [16, 17] from the feature map in the current layer. The second part denoted by ② is the main module in the DIA unit to model network attention and is the key innovation of the proposed method. Particularly, we apply Long Short-Term Memory (LSTM) [23] module that not only connects two adjacent layers, but also fuses attention from previous layers, creating nonlocal information communication throughout the DNN. Other network structures can also be explored to implement the second part and this is left as future work. The third part denoted by ③ adjusts (e.g., re-scaling or re-distributing) the feature map in the next layer according to the feedback of the second part.

Characteristics and Advantages. (1) As shown in Figure 1, the DIA unit is placed parallel to the network backbone, and it is shared with all the layers in the same stage (the collection of successive layers with same spatial size, as defined in [13]). It also links different layers implicitly and densely, which improves the interaction of layers at different depth. (2) As the DIA unit is shared, the number of parameter increment from the DIA unit remains roughly constant as the depth of the network increases. (3) DIA unit adaptively learns the non-local scaling that has the normalization effect.
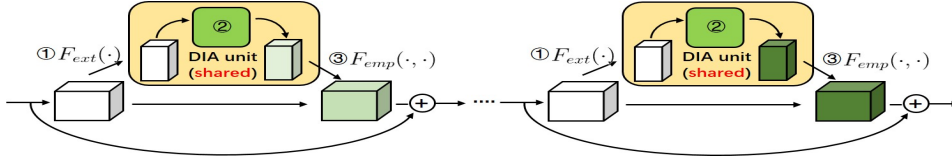

Figure 1: DIA units. F_{ext} means the operation for extracting different scales of features. F_{emp} means the operation for emphasizing features.

In this work, we focus on studying the DIA unit with modified LSTM, as shown in Figure 2. Three inputs are passed to the DIA unit: the extracted global information from current raw feature-map, the hidden state vector h_{t-1} and cell state vector c_{t-1} from previous layers. The modified LSTM can learn the channel-wise relationship and long distance dependency. Then it outputs the new hidden state vector h_t and the new cell state vector c_t. The cell state vector c_t stores the information from the tth layer and its preceding layers. The new hidden state vector h_t (dubbed as attention vector in our work) then applies back to the raw feature-map by channel-wise multiplication to emphasize the feature importance in each feature-map.

The LSTM plays a role as a bridge connecting the current layer and the preceding layers. The DIA unit with LSTM adaptively learns the non-linearity relationship between features in two different scales. The first scale of features is internal information of the current layer, and the second scale of features is outer information from the preceding layers. The diversity of this relationship will benefit attention modeling for current layer. Additionally, the operation of channel-wise multiplication in the final step of the DIA unit is similar to the scaling operation of Batch Normalization. Indeed the empirical results show that DIA has non-local normalization effect.

1.2 Organization

In Section 2, some of the attention-based networks are reviewed, and the difference between them and ours are discussed. Then in Section 3, the formal definition of Dense-and-Implicit Attention Network is introduced. In Section 4, we conduct experiments on Benchmarks datasets to empirically demonstrate the effectiveness of DIA unit. In Section 5, the influence of hyper-parameter on our model has been studied experimentally. Finally, in Section 6, some evidence of long-distance dependence in our model is shown, and the normalization effects of DIA unit are also investigated.
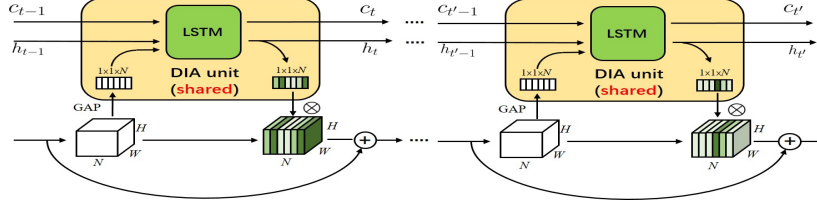
2

Figure 2: Illustration of DIANet with LSTM. In the LSTM module, c_t is the cell state vector and h_t is the hidden state vector. GAP means global average pool and $\otimes$ means channel-wise multiplication.

2 Related Works

Attention Mechanism in Computer Vision. [8] uses attention mechanism in image classification via utilizing a recurrent neural network to select and process local regions at high resolution sequentially, and this strategy also works for fine-grained image classification [24]. Concurrent attention-based methods tend to construct operation modules to capture non-local information in an image [18, 20], model the interrelationship between channel-wise features[15, 12]. The combination of multi-level attentions are also widely studied [17, 16, 25]. Unlike the prior works that the attention modules are inserted in each layer independently, in this work, the DIA unit is shared for all the layers throughout the networks, and the existing attention modules can be composited into the DIA unit readily.

Dense Network Topology. DenseNet proposed in [14] connects all pairs of layers directly with an identity map. Through the feature reuse, DenseNet enjoys the advantage of better parameter efficiency, the capacity of generalization, and more accessible training. Instead of explicit connection, DIA unit implicitly links the layers at different depth via a shared module and leads to dense connection. Empirical results in Section 6 shows that the DIA unit has a similar effect as DenseNet.

Multi-level Feature Integration. [26] experimentally analyzes that even the simple aggregation of low-level visual features sampled from wide inception field can be efficient and robust for context representation, which inspires [15, 12] to incorporate multi-level features to improve the network representation. [27] also demonstrates that by biasing the features response in each convolutional layers using different activation functions, the deeper layer could achieve the better capacity of capturing the abstract pattern in DNN. In DIA unit, the high non-linearity relationship between multi-scale features are learned and integrated via the LSTM module, which is conducive to better model the attention and improve learning performance reported in Section 4, 5 and 6.

3 Dense-and-Implicit Attention Network (DIANet)

In this section, we will formally introduce the DIA unit and elaborate on how it implicitly connects all the layers' attention densely. Note that in this section and later, we denote a neural network as DIANet if the network contains the DIA unit with the modified LSTM module.

3.1 Formulation of DIANet

Considering residual network [13] shown in Figure 2, we adopt the global average pooling to extract global information of features and the channel-wise multiplication to enhance the importance of features, which is similar to the components of SENet [15]. Formally, at t^{th} layer, the input of the LSTM is feature map $x_t \in \mathbb{R}^{W \times H \times N}$, where W, H, N means width, height and number of channels respectively. The residual mapping introduced in [13] is $f(\cdot; \theta_1^{(t)})$, where $\theta_1^{(t)}$ is the parameters at t^{th} layer. Then the output of residual is $a_t = f(x_t; \theta_1^{(t)}) \in \mathbb{R}^{W \times H \times N}$. Next, a_t will be applied with global average pooling (GAP$(\cdot)$) to extract global information from features in current layer. The output GAP$(a_t) \in \mathbb{R}^N$ will be passed into LSTM along with previous hidden state vector h_{t-1} and cell state vector c_{t-1} (h_0 and c_0 are zero vector initially). The LSTM will generate the current hidden state vector $h_t \in \mathbb{R}^N$, and cell state vector $c_t \in \mathbb{R}^N$ denoted as

$$h_t, c_t = \text{LSTM}(\text{GAP}(a_t), h_{t-1}, c_{t-1}; \theta_2). \tag{1}$$

The LSTM module will be used repeatedly and shared with different layers in parallel to the network backbone. Note that the number of parameters θ_2 in LSTM does not depend on the number of the backbone's layers, e.g., t. In our model, the hidden state vector h_t is regarded as attention

3

vector, the adaptive recalibration for feature maps. We apply channel-wise multiplication $\otimes$ to enhance the importance of features, and then obtain the output for the unit with skip connection, $x_{t+1} = x_t + a_t \otimes h_t$. For illustration purpose, Table 1 shows the formulation of ResNet, SENet, and DIANet. The main difference between them is the part (b). SENet utilizes the fully connected layer to model the channel-wise dependency [15], where the total number of parameters of the fully connected layers depends on the number of layers in the network backbone. In SENet, the total number of parameters $\theta_2^{(t)}$ over all the layers increases as the number of layers increases.

		ResNet	SENet	DIANet (ours)
(a)		$a_t = f(x_t; \theta_1^{(t)})$	$a_t = f(x_t; \theta_1^{(t)})$	$a_t = f(x_t; \theta_1^{(t)})$
(b)		-	$h_t = \text{FC}(\text{GAP}(a_t); \theta_2^{(t)})$	$h_t, c_t = \text{LSTM}(\text{GAP}(a_t), h_{t-1}, c_{t-1}; \theta_2)$
(c)		$x_{t+1} = x_t + a_t$	$x_{t+1} = x_t + a_t \otimes h_t$	$x_{t+1} = x_t + a_t \otimes h_t$

Table 1: Formulation for the structure of ResNet, SENet, and DIANet. f is the convolution layer. FC means fully connected layer and GAP indicates global average pooling over an input.

3.2 Modified LSTM Module (DIA-LSTM Module)

Now we introduce the modified LSTM module. As shown in Figure 3, comparing to the standard LSTM [23] module, we modify the LSTM with two modifications: 1) the shared linear transformation for input dimension reduction; 2) careful selection of activation function for better performance.

The standard LSTM shown in Figure 3 (Left) consists of four linear transformation layers. Since the input y_t, h_{t-1} and output h_t are of the same dimension, the standard LSTM may cause $8N^2$ parameters increment (see the Appendix). When the number of channels is large, e.g., $N = 2^{10}$, the parameters increment will be over 8 million, which can hardly be tolerated.
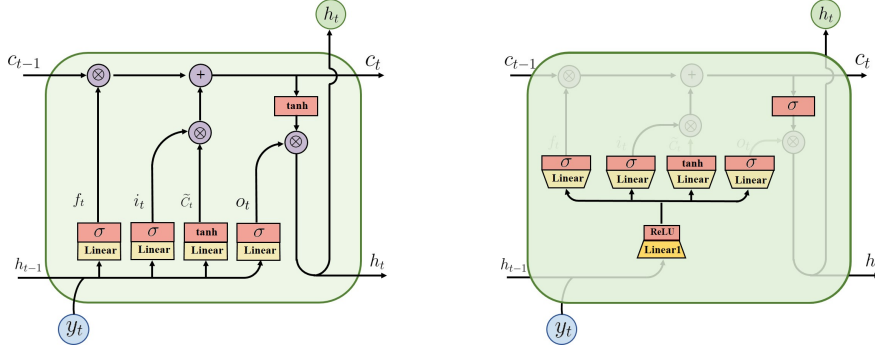

Figure 3: Left: Standard LSTM module. Right: Our modified LSTM module. σ means the sigmoid activation.

Hence, to avoid such a scenario, we propose a modified LSTM (denoted as DIA-LSTM) as follows:

(1) Activation Function We change the output layer's activation function from $tanh$ to $sigmoid$ and further discussion will be presented in ablation study;

(2) Parameter Reduction As shown in Figure 3 (Left), h_{t-1} and y_t will be used in four linear activation function which are three $sigmoid$ and one $tanh$ function. Then the outputs will be used for the input gate, forget gate and output gate. In DIA-LSTM, a linear transformation layer ("Linear1" in Figure 3 (Right)) with smaller output dimension will be applied to the h_{t-1} and y_t. We use reduction ratio r in the linear transformation layer. Specifically, we reduce the dimension of the input from $1 \times 1 \times N$ to $1 \times 1 \times {N}/{r}$ and then apply the $ReLU$ activation function to increase non-linearity in this module. The dimension of the output from $ReLU$ function will be changed back to $1 \times 1 \times N$ when the output is passed into those four linear transformation functions. This modification can enhance the relationship between the inputs for different gates in DIA-LSTM and also effectively reduce the number of parameters by sharing a linear transformation for dimension reduction. The number of parameter increment reduces from $8N^2$ to $10/r \times N^2$ (see the Appendix), and we found that when we choose appropriate reduction ratio r, we can make better trade-off between parameter

4

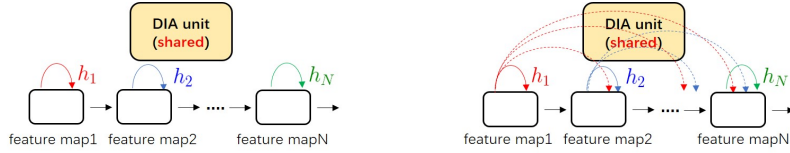reduction and the performance. Further experimental results will be discussed in the ablation study later.

Figure 4: (Left) Explicit structure of DIANet. (Right) Implicit Connection of DIA unit.

Implicit and Dense Connection. Now we illustrate how the DIA unit connects all the layers in the same stage densely. Consider a stage with many layers, as shown in Figure 4 (Left), it is an explicit structure of DIANet where the feature-map 1 seems not to connect with feature-map 2. However, the feature-map 1 and feature-map 2 share the same DIA unit and the memory part c_t in DIA-LSTM can memorize the information from feature-map 1 and use the information to model the attention. For these reasons, the DIA-LSTM, regarded as the bridge, implicitly propagates information forward from feature-map 1 to feature-map 2. As shown in Figure 4 (Right) that there is an implicit connection adding between feature-map 1 and feature-map 2. Similarly, when the DNN has many layers as network depth increases, in each stage the DIA-LSTM will sequentially receive feature map from different layers, and in each time-step the information from all the previous layers will be incorporated to model the attention for current layer's feature-map.

4 Experiments

In this section, we evaluate the performance of DIA unit in image classification task and empirically demonstrate its effectiveness. We conduct experiments on popular networks for benchmark datasets. Similarly, the SENet [15] is also channel-specific attention model, we compare DIANet with SENet. To fairly compare with SENet, we adjust the reduction ratio such that the number of parameters of DIANet is similar to that of SENet.

Dataset and Model. We conduct experiments on CIFAR10, CIFAR100 [28], and ImageNet 2012 [29] using ResNet [13], PreResNet [30], WRN [31] and ResNeXt [32]. CIAFR10 or CIFAR100 has 50k train images and 10k test images of size 32 by 32, but has 10 and 100 classes respectively. ImageNet 2012 dataset[29] comprises 1.28 million training and 50k validation images from 1000 classes, and the random cropping of size 224 by 224 is used in our experiments. The implementation details can be found in the appendix.

Image Classification. As shown in Table 2, DIANet improves the testing accuracy significantly over the original networks and consistently comparing with SENet for different datasets. In particular, the improvement of the ResNet performance is most remarkable. Due to the popularity of ResNet, DIA unit may be applied in other computer vision tasks.

	Dataset	original		SENet		DIANet		
		#P(M)	top1-acc.	#P(M)	top1-acc.	#P(M)	top1-acc.	r
ResNet164	CIFAR100	1.73	73.43	1.93	75.03	1.95	**76.67**	4
PreResNet164	CIFAR100	1.73	76.53	1.92	77.41	1.96	**78.20**	4
WRN52-4	CIFAR100	12.07	79.75	12.42	80.35	12.30	**80.99**	4
ResNext101,8x32	CIFAR100	32.14	81.18	34.03	82.45	33.01	**82.46**	4
ResNet164	CIFAR10	1.70	93.54	1.91	94.27	1.92	**94.58**	4
PreResNet164	CIFAR10	1.70	95.01	1.90	95.18	1.94	**95.23**	4
WRN52-4	CIFAR10	12.05	95.96	12.40	95.95	12.28	**96.17**	4
ResNext101,8x32	CIFAR10	32.09	95.73	33.98	96.09	32.96	**96.24**	4
ResNet34	ImageNet	21.81	73.93	21.97	74.39	21.98	**74.60**	20
ResNet50	ImageNet	25.58	76.01	28.09	76.61	28.38	**77.24**	20
ResNet152	ImageNet	60.27	77.58	66.82	78.36	65.85	**78.87**	20
ResNext50,32x4	ImageNet	25.03	77.19	27.56	78.04	27.83	**78.32**	10

Table 2: Testing accuracy (%) on CIFAR10, CIFAR100 and ImageNet 2012. "#P(M)" means the number of parameters (million). The rightmost "r" indicates the compression ratio of DIANet.

5 Ablation Study

In this section, we conduct ablation experiment to explore how to better embed DIA unit in different neural network structures and gain a better understanding of the role of each component in the DIA unit. All ablation experiments are performed on CIFAR-100 dataset with ResNet. First we discuss the effect of the reduction ratio r introduced in DIA-LSTM ,i.e., Figure 3 (Right). Then the performance of DIA unit in ResNet of different lengths will be explored. We test the performance of DIA-LSTM with different activation function at output layer. Also, we study the capacity of the stacked DIA-LSTM with different number of DIA-LSTM modules.

Reduction ratio. The reduction ratio rate is the only hyperparameter in our DIANet, as mentioned in Section 3.2. Improving the performance with light parameter increment is one of the main characteristic in our model. This part investigates the trade-off between model complexity and its performance. As shown in Table 3, we find out that the testing accuracy of DIANet will decline slightly with the increasing reduction rate. In particular, when $r = 16$, the increment of parameters is 0.05M comparing with ResNet164. The testing accuracy of DIANet is 76.50% while that of the original network is 73.43% which makes DIA unit has great potential in a variety of practical applications, especially those in which small model size is of importance.

DIANet				CIFAR-100	SENet		DIANet($r = 4$)	
Ratio r	#P(M)	top1-acc.		Depth	#P(M)	top1-acc.	#P(M)	top1-acc.
1	$2.59_{(+0.86)}$	76.88		ResNet83	0.99	74.67	$1.11_{(+0.12)}$	75.02
4	$1.95_{(+0.22)}$	76.67		ResNet164	1.93	75.03	$1.95_{(+0.02)}$	76.67
8	$1.84_{(+0.11)}$	76.42		ResNet245	2.87	75.03	$2.78_{(-0.09)}$	76.79
16	$1.78_{(+0.05)}$	76.50		ResNet407	4.74	75.54	$4.45_{(-0.29)}$	76.98

Table 3: Test accuracy (%) with varying reduction ratio on CIFAR100. Table 4: Test accuracy (%) with models of different depth on CIFAR100.

The depth of the neural network. Generally, in practice deep DNNs with large amount of parameters do not guarantee sufficient performance improvement since, on the one hand, deeper networks will probably contain extreme features and parameters redundancy [14]. On the other hand, the gradient degradation problem will be worse and make the DNN hard to be trained [33, 34, 35]. Therefore, prior works in designing new structure of deep neural networks [13, 14, 35] like ResNet[13] and DenseNet[14] and embed attention modules to enhance the network performance like SENet[15] are of great necessity. In order to evaluate the effectiveness of DIANet structure encountering deep networks, we investigate how the depth of the DNN influence the DIANet in two parts: (1) the performance of DIANet compared to SENet of varying depth; (2) the parameter increment of DIANet in DNN. The results in Table 4 show that as the depth of the ResNet increases from 83 layers to 407 layers, the DIANet can achieve higher classification accuracy improvement than the SENet. Moreover, DIANet83 (for simplicity, 83 denotes the depth ResNet backbone) can achieve the competitive result as SENet164, and DIANet164 can outperform all the SENet results with at least 1.13% and at most 58.8% parameter reduction. They implies that the DIANet is of higher parameter efficiency than SENet. The results also suggest that: for DIANet, as shown in Figure 2, the deeper network means that the DIA-LSTM module will pass much more layers in the same stage recurrently. The DIA-LSTM can handle the interrelationship between different layer's information in much deeper DNN and adaptively emphasis the previous inputs that are most correlated to the current input. Therefore the DIANet can effectively avoid learning redundancy.

	#P(M)	Activation	#DIA-LSTM	top1-acc.
ResNet164	1.95	sigmoid	1	76.67
ResNet164	1.95	tanh	1	75.24
ResNet164	3.33	sigmoid	3	75.20
ResNet164	3.33	tanh	3	76.47

Table 5: Test accuracy (%) on CIFAR100. The effect of activation function at the output layer in DIA-LSTM and the number of staking DIA-LSTM modules.

Activation function and number of DIA-LSTM. We choose two different activation functions ($sigmoid$ and $tanh$) in DIA-LSTM's output layer and two different number(one and three) of stacking DIA-LSTM cells to explore the effects of these two factors on classification performance. In

Table 5, we find that the performance has been greatly improved after replacing $tanh$ with $sigmoid$. As shown in Figure 3(Right), this activation function is located in the output layer, which directly changes the effect of memory unit c_t on the output of the output gate.

When we use $sigmoid$ in DIA-LSTM's output layer, An increasing number of stacking DIA-LSTM modules do not necessarily lead to performance improvement but may lead to more considerable performance degradation. However, when we choose $tanh$, the situation is different. It suggests that for the DIA unit to be effective, fine structural adjustments are necessary.

6 Analysis

This section studies some properties of DIANe including features integration and normalization effect. In DIANet, the deeper layers connect the shallower layers via DIA-LSTM module. Firstly, the random forest model [36] is used to interpret how the current layer depends on the preceding layers. Secondly, we study the normalization effect of DIANet by removing the Batch Normalization [37] in the networks. Also, we investigate some positive side-effects of DIA.

Features Integration. Here we try to understand the dense connection from the numerical perspective. As shown in Figure 2 and 4, the DIA-LSTM, playing a role as a bridge, propagates the information forward through h_t and c_t. Moreover, h_t at different layers are also integrating with $h_{t'}, 1 \leq t' < t$ in DIA-LSTM. Notably, h_t will apply directly to the features in the network at each layer t. Therefore the relationship between h_t at different layers somehow reflects connection degree of different layers. We explore the nonlinear relationship between the hidden state h_t of DIA-LSTM and the preceding hidden state $h_{t-1}, h_{t-2}, ..., h_1$, and study how the information coming from $h_{t-1}, h_{t-2}, ..., h_1$ contribute to h_t. To reveal this relationship, we consider using the random forest to measure variable importance. The random forest can return the input variables' contribution to the output separately in the form of importance measure, e.g., Gini importance [36]. The computation details of Gini importance can be referred to the Appendix. Take $h_n, 1 \leq n < t$ as input variables and h_t as output variable, we find out the Gini importance of each variable $h_n, 1 \leq n < t$. ResNet164 contains three stages, and each stage consists of 18 layers. We conduct three Gini importance computation to each stage separately. As shown in Figure 5, each row presents the importance of source layers $h_n, 1 \leq n < t$ contributing to the target layer h_t. In each sub-graph of Figure 5, the diversity of variable importance distribution indicates that the current layer utilizes the information of the preceding layers. The interaction between shallow and deep layers in the same stage reveals the effect of implicitly dense connection. In particular, taking h_{17} in stage 1 (the last row) as an example, h_{16} or h_{15} does not intuitively provide the most information for h_{17}, but h_5 does. We conclude that the DIA unit can adaptively integrate information between multiple layers.
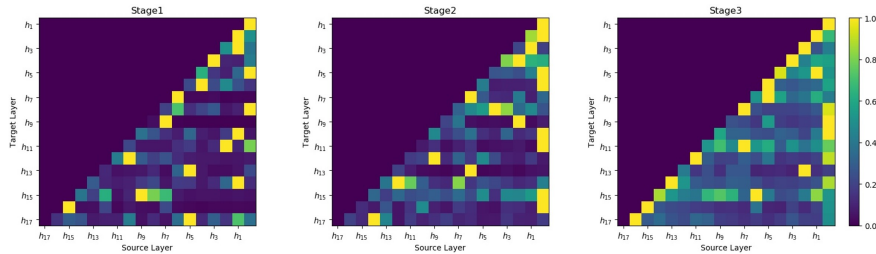

Figure 5: Features integration for each stage.

Moreover, in Figure 5(stage 3), the information interaction with previous layers in stage 3 are more intense and frequent than that of the first two stages. Correspondingly, as shown in Table 6(Left), in the experiments when we remove the DIA unit in stage 3, the classification accuracy decreases from 76.67 to 75.40. However, when it in stage 1 or 2 is removed, the performance degradation is very similar, falling to 76.27 and 76.25 respectively. Also note that for DIANet, the number of parameters increment in stage 2 is much larger than that of stage 1. It implies that the significant performance degradation after the removal of stage 3 may be not only due to the reduction of the number of parameters but also due to the lack of dense feature integration.

Normalization Effect of DIANet. Small changes in shallower hidden layers may be amplified as the information propagates within the deep architecture and sometimes result in a numerical explosion.

	#P(M)	#P(M)↓	top1-acc.	top1-acc.↓
stage1	1.94	0.01	76.27	0.40
stage2	1.90	0.05	76.25	0.42
stage3	1.78	0.17	75.40	1.27

Models	CIFAR-10	CIFAR-100
ResNet164	87.32	60.92
SENet	88.30	62.91
DIANet	**89.25**	**66.73**

Table 6: (Left) The effect of removal of DIA units in different stage. We test on CIFAR100 with ResNet164. (Right) Test accuracy (%) of the models without data augment.

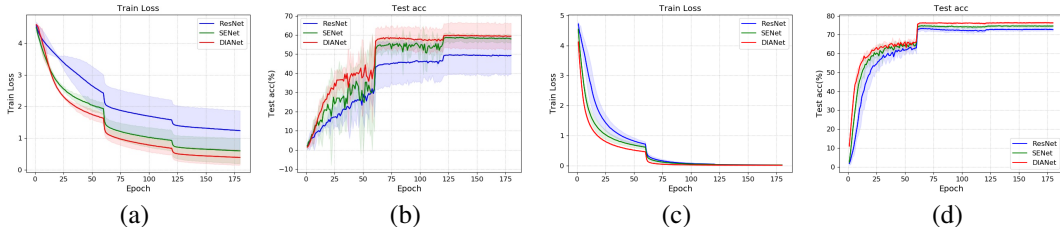(a)   (b)   (c)   (d)

Figure 6: (a-b) and (c-d) are the performance of three kinds of network without and with the last one-thirds of the skip connections at each stage, respectively.Testing with ResNet164 and CIFAR-100.

Batch Normalization (BN) [37] is widely used in the modern deep networks since it stabilizes the training by standardizing the input of each layer. DIA unit readjusts the feature maps by channel-wise multiplication, which plays a role of scaling similar to BN. In this part, we empirically claim that DIA unit has a normalization effect. As shown in Table 7, different models trained with varying depth in CIFAR-100, and BNs are removed in these networks to eliminate their normalization effect. The experiments are conducted on a single GPU with batch size 128 and initial learning rate 0.1. Both the original ResNet, SENet face problem of numerical explosion without BN while the DIANet can be trained with depth up to 245. Besides, comparing with Table 4, the testing accuracy of DIANet without BN still can keep up to 70%. The difference between the performance of the network with BN and network with BN and DIA indicates that the normalization effect of BN and that of DIANet is different. BN learns the shift and the scaling parameters by utilizing the local information, i.e., current layer and batch data. However, the scaling learned by DIANet integrates the information from preceding layers and enables the network to choose a better scaling for each mapping. Combination of BN and DIANet can learn the local scaling, but also the non-local scaling.

	original		SENet		DIANet($k = 16$)	
	#P(M)	top1-acc.	#P(M)	top1-acc.	#P(M)	top1-acc.
ResNet83	0.88	nan	0.98	nan	0.94	**70.58**
ResNet164	1.70	nan	1.91	nan	1.76	**72.36**
ResNet245	2.53	nan	2.83	nan	2.58	**72.35**
ResNet326	3.35	nan	3.75	nan	3.41	nan

Table 7: Testing accuracy (%). We train models of different depth without BN on CIFAR-100. "nan" indicates the numerical explosion.

Removal of skip connection. The skip connections have become a necessary operation for training the DNN [30]. Without skip connection, the DNN is hard to train due to some reasons like the gradient vanishing. Figure 6(a-b) shows the training curves if we remove the last one-third of the skip connections at each stage. We can find that the decline of train loss in DIANet is more stable and DIANet achieves a smaller training loss. At the same time, DIANet has higher test accuracy than SENet and original ResNet. To some extent, it shows that DIA unit can alleviate the gradient vanishing in deep network training.

Without data augment. Explicit dense connections may help bring more efficient usage of parameters, which makes the neural network less prone to overfit [14]. Although the dense connections in DIA are implicit, the DIANet still shows the ability to reduce overfitting. To verify it, We train the models without data augment to reduce the influence of regularization from data augment. As shown in Table 6 (Right), DIANet achieves lower testing error than ResNet164 and SENet. To some extent, the implicit and dense structure of DIANet may have regularization effect.

7   Conclusion

In this paper, we proposed a Dense-and-Implicit Attention (DIA) unit to enhance the generalization capacity of deep neural networks by recurrently fusing feature attention throughout different layers. Experiments showed that the DIA unit could be universally applied to different network architectures and improve their performance. The DIA unit is also supported by empirical analysis and extensive ablation study. Notably, the DIA unit can be constructed as a global networks module and can implicitly change the topology of existing network backbones.

References

[1] John R Anderson. *Cognitive psychology and its implications*. Macmillan, 2005.

[2] Kelvin Xu, Jimmy Lei Ba, Ryan Kiros, Kyunghyun Cho, Aaron Courville, Ruslan Salakhutdinov, Richard S. Zemel, and Yoshua Bengio. Show, attend and tell: Neural image caption generation with visual attention. In *Proceedings of the 32Nd International Conference on International Conference on Machine Learning - Volume 37*, ICML'15, pages 2048–2057. JMLR.org, 2015.

[3] Minh-Thang Luong, Hieu Pham, and Christopher D Manning. Effective approaches to attention-based neural machine translation. *arXiv preprint arXiv:1508.04025*, 2015.

[4] Ashish Vaswani, Noam Shazeer, Niki Parmar, Jakob Uszkoreit, Llion Jones, Aidan N Gomez, Łukasz Kaiser, and Illia Polosukhin. Attention is all you need. In *Advances in neural information processing systems*, pages 5998–6008, 2017.

[5] Denny Britz, Anna Goldie, Minh-Thang Luong, and Quoc Le. Massive exploration of neural machine translation architectures. *arXiv preprint arXiv:1703.03906*, 2017.

[6] Jianpeng Cheng, Li Dong, and Mirella Lapata. Long short-term memory-networks for machine reading. *EMNLP 2016*, 2016.

[7] Antoine Miech, Ivan Laptev, and Josef Sivic. Learnable pooling with context gating for video classification. *arXiv preprint arXiv:1706.06905*, 2017.

[8] Volodymyr Mnih, Nicolas Heess, Alex Graves, et al. Recurrent models of visual attention. In *Advances in neural information processing systems*, pages 2204–2212, 2014.

[9] Dzmitry Bahdanau, Kyunghyun Cho, and Yoshua Bengio. Neural machine translation by jointly learning to align and translate. *arXiv preprint arXiv:1409.0473*, 2014.

[10] Alejandro Newell, Kaiyu Yang, and Jia Deng. Stacked hourglass networks for human pose estimation. In *European Conference on Computer Vision*, pages 483–499. Springer, 2016.

[11] Peter Anderson, Xiaodong He, Chris Buehler, Damien Teney, Mark Johnson, Stephen Gould, and Lei Zhang. Bottom-up and top-down attention for image captioning and visual question answering. In *Proceedings of the IEEE Conference on Computer Vision and Pattern Recognition*, pages 6077–6086, 2018.

[12] Jie Hu, Li Shen, Samuel Albanie, Gang Sun, and Andrea Vedaldi. Gather-excite: Exploiting feature context in convolutional neural networks. In *Advances in Neural Information Processing Systems*, pages 9401–9411, 2018.

[13] Kaiming He, Xiangyu Zhang, Shaoqing Ren, and Jian Sun. Deep residual learning for image recognition. In *Computer Vision and Pattern Recognition*, 2016.

[14] Gao Huang, Zhuang Liu, Kilian Q Weinberger, and Laurens van der Maaten. Densely connected convolutional networks. In *Computer Vision and Pattern Recognition*, 2017.

[15] Jie Hu, Li Shen, and Gang Sun. Squeeze-and-excitation networks. In *Proceedings of the IEEE conference on computer vision and pattern recognition*, pages 7132–7141, 2018.

[16] Sanghyun Woo, Jongchan Park, Joon-Young Lee, and In So Kweon. Cbam: Convolutional block attention module. In *Proceedings of the European Conference on Computer Vision (ECCV)*, pages 3–19, 2018.

[17] Jongchan Park, Sanghyun Woo, Joon-Young Lee, and In So Kweon. Bam: Bottleneck attention module. *arXiv preprint arXiv:1807.06514*, 2018.

[18] Xiaolong Wang, Ross Girshick, Abhinav Gupta, and Kaiming He. Non-local neural networks. In *Proceedings of the IEEE Conference on Computer Vision and Pattern Recognition*, pages 7794–7803, 2018.

[19] Xiang Li, Wenhai Wang, Xiaolin Hu, and Jian Yang. Selective kernel networks. 2019.

[20] Yue Cao, Jiarui Xu, Stephen Lin, Fangyun Wei, and Han Hu. Gcnet: Non-local networks meet squeeze-excitation networks and beyond. *arXiv preprint arXiv:1904.11492*, 2019.

[21] Wenhai Wang, Xiang Li, Jian Yang, and Tong Lu. Mixed link networks. *arXiv preprint arXiv:1802.01808*, 2018.

[22] Max Jaderberg, Karen Simonyan, Andrew Zisserman, et al. Spatial transformer networks. In *Advances in neural information processing systems*, pages 2017–2025, 2015.

[23] Sepp Hochreiter and Jürgen Schmidhuber. Long short-term memory. *Neural computation*, 9(8):1735–1780, 1997.

[24] Bo Zhao, Xiao Wu, Jiashi Feng, Qiang Peng, and Shuicheng Yan. Diversified visual attention networks for fine-grained object classification. *IEEE Transactions on Multimedia*, 19(6):1245–1256, 2017.

[25] Xudong Wang, Zhaowei Cai, Dashan Gao, and Nuno Vasconcelos. Towards universal object detection by domain attention. *CoRR*, abs/1904.04402, 2019.

[26] Lior Wolf and Stanley Bileschi. A critical view of context. *International Journal of Computer Vision*, 69(2):251–261, 2006.

[27] Hongyang Li, Wanli Ouyang, and Xiaogang Wang. Multi-bias non-linear activation in deep neural networks. In *International conference on machine learning*, pages 221–229, 2016.

[28] Alex Krizhevsky and Geoffrey Hinton. Learning multiple layers of features from tiny images. Technical report, Citeseer, 2009.

[29] Olga Russakovsky, Jia Deng, Hao Su, Jonathan Krause, Sanjeev Satheesh, Sean Ma, Zhiheng Huang, Andrej Karpathy, Aditya Khosla, Michael Bernstein, Alexander C. Berg, and Li Fei-Fei. ImageNet Large Scale Visual Recognition Challenge. *International Journal of Computer Vision (IJCV)*, 115(3):211–252, 2015.

[30] Kaiming He, Xiangyu Zhang, Shaoqing Ren, and Jian Sun. Identity mappings in deep residual networks. In *European Conference on Computer Vision*, 2016.

[31] Sergey Zagoruyko and Nikos Komodakis. Wide residual networks. In *BMVC*, 2016.

[32] Saining Xie, Ross Girshick, Piotr Dollár, Zhuowen Tu, and Kaiming He. Aggregated residual transformations for deep neural networks. In *Computer Vision and Pattern Recognition*, 2017.

[33] Yoshua Bengio, Patrice Simard, Paolo Frasconi, et al. Learning long-term dependencies with gradient descent is difficult. *IEEE transactions on neural networks*, 5(2):157–166, 1994.

[34] Xavier Glorot and Yoshua Bengio. Understanding the difficulty of training deep feedforward neural networks. In *Proceedings of the thirteenth international conference on artificial intelligence and statistics*, pages 249–256, 2010.

[35] Rupesh K Srivastava, Klaus Greff, and Jürgen Schmidhuber. Training very deep networks. In *Advances in neural information processing systems*, pages 2377–2385, 2015.

[36] Baptiste Gregorutti, Bertrand Michel, and Philippe Saint-Pierre. Correlation and variable importance in random forests. *Statistics Computing*, 27(3):659–678, 2017.

[37] Sergey Ioffe and Christian Szegedy. Batch normalization: Accelerating deep network training by reducing internal covariate shift. In *Proceedings of the 32Nd International Conference on International Conference on Machine Learning - Volume 37*, ICML'15, pages 448–456. JMLR.org, 2015.

[38] The computational work for this article was partially performed on resources of the national supercomputing centre, singapore (https://www.nscc.sg).

A Introdcution of Implementation detail

	ResNet164	PreResNet164	WRN52-4	ResNext101-8x32
Batch size	128	128	128	128
Epoch	180	164	200	300
Optimizer	SGD(0.9)	SGD(0.9)	SGD(0.9)	SGD(0.9)
depth	164	164	52	101
schedule	60/120	81/122	80/120/160	150/225
wd	1.00E-04	1.00E-04	5.00E-04	5.00E-04
gamma	0.1	0.1	0.2	0.1
widen-factor	-	-	4	4
cardinality	-	-	-	8
lr	0.1	0.1	0.1	0.1
$F_{ext}(\cdot)$	GAP	BN+GAP	BN+GAP	GAP
drop	-	-	0.3	-

Table 8: Implementation detail for **CIFAR10/100** image classification. Normalization and standard data augmentation (random cropping and horizontal flipping) are applied to the training data. GAP and BN denote Global Average Pooling and Batch Normalization separately.

	ResNet34	ResNet50	ResNet152	ResNext50-32x4
Batch size	256	256	256	256
Epoch	120	120	120	120
Optimizer	SGD(0.9)	SGD(0.9)	SGD(0.9)	SGD(0.9)
depth	34	50	152	50
schedule	30/60/90	30/60/90	30/60/90	30/60/90
wd	1.00E-04	1.00E-04	5.00E-04	5.00E-04
gamma	0.1	0.1	0.2	0.1
widen-factor	-	-	4	4
cardinality	-	-	-	8
lr	0.1	0.1	0.1	0.1
$F_{ext}(\cdot)$	GAP	GAP	GAP	GAP
drop	-	-	0.3	-

Table 9: Implementation detail for **ImageNet 2012** image classification. Normalization and standard data augmentation (random cropping and horizontal flipping) are applied to the training data. The random cropping of size 224 by 224 is used in these experiments. GAP denote Global Average Pooling .

Batch size	train batchsize
Epoch	number of total epochs to run
Optimizer	Optimizer
depth	the depth of the network
schedule	Decrease learning rate at these epochs
wd	weight decay
gamma	learning rate is multiplied by gamma on schedule
widen-factor	Widen factor
cardinality	Model cardinality (group)
lr	initial learning rate
$F_{ext}(\cdot)$	extract features(Figure 1)
drop	Dropout ratio

Table 10: The Additional explanation

B   Gini importance

Algorithm 1 Calculate features integration by Gini importance from Random Forest

---

Input: H: composed of $h_1,h_2,...,h_t$ from stage i;
       #The size of H is $(b_z \times c_z \times f_z)$
       #b_z denotes the batch size of h_t
       #c_z denotes the number of the feature maps' channel in current stage
       #f_z denotes the number of layers in current stage
Output: The hotmap G about the features integration for stage i;
 1: initial $G = \emptyset$;
 2: **for** $j = 1$ to $f_z - 1$ **do**
 3:    $x \leftarrow [h_1, h_2, ..., h_{j-1}]$;
 4:    $y \leftarrow [h_j]$;
 5:    $x \leftarrow x.\text{reshape}(b_z,(f_z - j) \times c_z)$;
 6:    RF $\leftarrow$ RandomForestRegressor();
 7:    RF.fit(x,y);
 8:    Gini_importances $\leftarrow$ RF.feature_importances_;
       #The length of Gini_importance is $(f_z - j) \times c_z$
 9:    res $\leftarrow \emptyset$;
10:    $s \leftarrow 0$;
11:    cnt $\leftarrow 0$;
12:    **for** $k = 0$ to $(f_z - j)$ **do**
13:       $s \leftarrow s +$ Gini_importance(k);
14:       cnt $\leftarrow$ cnt + 1;
15:       **if** cnt == c_z-1 **then**
16:          res.add(s);
17:          $s \leftarrow 0$;
18:          cnt $\leftarrow 0$;
19:       **end if**
       G.add(res/$\max$(res));
20:    **end for**
21: **end for**

C   Number of parameter of LSTM

Suppose the input y_t is of size N and the hidden state vector h_{t-1} is also of size N.

Standard LSTM As shown in Figure (3) (Left), in the standard LSTM, there requires 4 linear transformation to control the information flow with input y_t and h_{t-1} respectively. The output size is set to be N. To simplify the calculation, the bias is omitted. Therefore, for the y_t, the number parameters of 4 linear transformation is equal to $4 \times n \times n$. Similarly, the number parameters of 4 linear transformation with input h_{t-1} is equal to $4 \times n \times n$. The total of parameters equals to $8n^2$.

DIA-LSTM As shown in Figure (3) (Right), there is a linear transformation to reduce the dimension at the beginning. The dimension of input y_t will reduce from N to N/r after the first linear transformation. The number of parameters for the linear transformation is equal to $n \times n/r$. Then the output will be passed into 4 linear transformation same as the standard LSTM. the number parameters of 4 linear transformation is equal to $4 \times n/r \times n$. Therefore, for input y_t and reduction ratio r, the number of parameters is equal to $5n^2/r$. Similarly, the number of parameters with input h_{t-1} is the same as that concerning y_t. The total of parameters equals to $10n^2/r$.